International Journal of Agriculture and Biosciences 2025 xx(x): xx-xx.
https://doi.org/10.47278/journal.ijab/2025.078

RESEARCH ARTICLE

eISSN: 2306-3599; pISSN: 2305-6622

Potential use of Graphene-Like Nanomaterials in Soil Sensors and Moisture Monitoring

M.K. Kazankapova, B.T. Yermagambet*, B.K. Kasenov, A.B. Malgazhdarova, Zh.T. Dauletzhanova, Zh.M. Kassenova, G.K. Mendaliyev and A.S. Akshekina

LLP "Institute of Coal Chemistry and Technology," 010013 Astana, Kazakhstan
*Corresponding author: B.T.Yermagambet@outlook.com

ABSTRACT

Advancing precision agriculture requires materials that enhance the performance and sensitivity of soil-monitoring technologies. This study explores the synthesis and characterization of graphene-like carbon nanomaterials obtained via arc discharge method, assessing their suitability for use in agricultural soil sensors and moisture detection systems. Graphene-based nanomaterials were synthesized using graphite electrodes in an inert nitrogen atmosphere under arc discharge conditions at 75V with variable current strengths (50–400A). The synthesized materials were characterized using Raman spectroscopy, SEM, and BET surface area analysis. Their electrophysical properties including dielectric permittivity, electrical resistance and conductivity were evaluated across a temperature range of 293–483K and frequencies of 1, 5, and 10kHz. The synthesized nanomaterials demonstrated multilayer graphene structures with high degrees of graphitization and long-range order, verified by characteristic 2D Raman peaks. SEM imaging revealed flake-like graphene morphology with high specific surface areas (up to 159.7m^2/g). Dielectric permittivity values exceeded 10^8 at elevated temperatures, and the materials showed semiconductor behavior across the measured range. These properties suggest strong potential for enhancing sensitivity and performance in soil moisture and conductivity sensors. Graphene-like nanomaterials produced via arc discharge exhibit the structural, electrical, and thermal stability necessary for application in agricultural sensing devices. Their high permittivity and conductivity make them excellent candidates for integration into soil moisture monitoring systems, contributing to more efficient water use and improved crop management in precision agriculture.

Keywords: Graphene, Arc Discharge, Graphite, Carbon Nanomaterials (CNMs), Carbon Nanotubes (CNTs).

Article History
Article # 25-208
Received: 23-Apr-25
Revised: 11-May-25
Accepted: 14-May-25
Online First: 24-May-25

INTRODUCTION

In the light of the transition to a "green economy" (Baibussenov 2023; Markhayeva et al., 2023) and the gradual phase-out of coal as a fuel (Mazina et al., 2022), there is a need to transform hydrocarbon raw materials into more environment friendly sources of energy (Bugubaeva et al., 2023). Simultaneously, there is a need to increase the added value of hydrocarbon products. One example of such a product is multilayered graphite material similar to graphene, made as a result of prolonged mechanochemical activation of coal.

This irreversible activation process sequentially changes the chemical composition, physical, and technological properties of activated and coked coals during their transformation into multilayered graphene, representing a carbon metamorphosis. Structural-molecular restructuring of activated and coked coals is accompanied by an increase in the relative carbon content, a decrease in oxygen content, and the release of volatile substances. Changes also occur in hydrogen content, combustion heat, hardness, density, brittleness, optical, electrical, and other physical properties (Yermagambet et al., 2021).

Cite this Article as: Kazankapova MK, Yermagambet BT, Kasenov BK, Malgazhdarova AB, Dauletzhanova ZT, Kassenova ZM, Mendaliyev GK and Akshekina AS, 2025. Potential use of graphene-like nanomaterials in soil sensors and moisture monitoring. International Journal of Agriculture and Biosciences xx(x): xx-xx. https://doi.org/10.47278/journal.ijab/2025.078

A Publication of Unique Scientific Publishers

In recent years, the growing demand for high-speed electronics (Nosova et al., 2018) and renewable energy (Abdullayev et al., 2023) sources have stimulated researchers to discover, develop and assemble new classes of nanomaterials (Tulepova et al., 2024). Among these materials, carbon-based nanomaterials have attracted special attention due to their unique structural and physical properties. Carbon nanomaterials, consisting entirely of sp2-bonded graphitic carbon, exist in all reduced dimensions, including zero-dimensional fullerenes, one-dimensional carbon nanotubes (CNTs), and two-dimensional graphene (Hersam, 2008; Allen et al., 2010; Jariwala et al., 2011). Characteristics of different carbon nanomaterials are presented in Table 1.

These carbon nanomaterials exhibit diverse properties and have applications across various fields, including electronics, energy, medicine and environmental remediation. The development of graphene production methods is becoming increasingly relevant due to the unique properties of this material, which make it attractive for a multitude of applications. Important characteristics of graphene include its high electrical conductivity, thermal conductivity, transparency, mechanical strength, and chemical stability (Rao et al., 2009; Raccichini et al., 2014). Many of these properties are due to its electronic structure: graphene is a gapless semimetal, and its charge carriers are massless Dirac fermions (Shavelkina et al., 2019). As a result, there is a significant demand for graphene in various fields, including energy (solar cells, batteries, hydrogen storage) (Georgakilas et al., 2016), ceramic materials science (Palmero et al., 2014), polymers (King et al., 2013), metals (Gupta et al., 2016), biotechnology and other nanocomposites (Palmero et al., 2014).

The main factors contributing to the increased consumption of graphene are as follows: 1) the rapid growth in the number of graphene producers and their derivatives; 2) the increasing utilization of graphene-based products in various economic sectors; 3) heightened interest in scientific research in the field of sorbents. High demand and universal application of graphene create a need for synthesis of new materials similar to it in structure. Graphene nanosheets were first isolated in 2004 by Andre Geim and Konstantin Novoselov (Kong et al., 2009; Dreyer et al., 2010). These researchers also experimentally obtained monolayer graphene by micromechanical cleavage of graphite using the "Scotch tape" method. The extraordinary expectations surrounding graphene stem from its unparalleled physical and chemical properties. Structurally, graphene consists of a single layer of carbon atoms arranged in a two-dimensional hexagonal lattice, with a thickness of approximately 70picometers equivalent to about one-millionth the diameter of a human hair (Eda et al., 2008). Graphene is considered the thinnest and lightest material, weighing 0.77mg/m^2. It is also one of the strongest materials, with a Young's modulus of around ~1000GPa and a tensile strength of 130GPa (Benayad et al., 2009). The elasticity modulus of graphene is about ~0.25TPa (Nie et al., 2003) and its thermal conductivity reaches approximately ~5,000 W/m.K (Naik et al., 2011). For comparison, the thermal conductivity of copper is 400 W/m·K. Graphene exhibits high gas impermeability, including to helium, and has high electrical conductivity of about ~2,000,000 cm^2/V·s, corresponding to 200S/m^2·K (Kratschmer et al., 1990; Ji et al., 2012). Its melting temperature exceeds 3000°C.

In early studies on the synthesis of fullerenes and graphene, high-purity graphite was used as a precursor. After obtaining gram quantities of fullerenes (C60) in 1990 (Richter et al., 1997), new nanoscale carbon materials were discovered, such as carbon nanotubes, higher fullerenes (Ugarte, 1992), carbon onion nanostructures (Yudasaka et al., 2008), carbon nanohorns, and nanocones (Zhang et al., 2001), bamboo-like carbon nanotubes (Du et al., 2008), graphene, and other nanomaterials. Graphite represents the most stable form of pure carbon at standard pressure and temperature, and its structure was determined by John Desmond Bernal in 1924 (Balandin et al., 2008). Therefore, graphite is the most common form encountered as coal.

The bonds within the planes of graphite are covalent, while the interplanar bonds are weak van der Waals interactions, making graphite susceptible to fracture. Carbon has a tetrahedral structure, where in its hexagonal lattice, it is covalently bonded to only three neighbors. The fourth valence electron forms weakly localized π-bonds with its neighbors in the same plane. This last electron can participate in the conductivity of graphite, but mainly within the plane (Kazankapova et al., 2020). Regarding carbon nanomaterials' environmental value, technologies

Table 1: Characteristics of Carbon Nanomaterials

Material	Structure	Properties	Application
Graphene	Single layer of carbon atoms arranged in a two-dimensional honeycomb lattice	Exceptional mechanical strength, high electrical conductivity, high thermal conductivity, transparency, and flexibility	Flexible electronics, transparent conductive films, sensors, composite materials, energy storage, and biomedical devices
Carbon Nanotubes (CNTs)	Cylindrical nanostructures composed of rolled-up graphene sheets	High tensile strength, excellent electrical and thermal conductivity, flexibility, and high aspect ratio	Field-effect transistors, conductive polymers, nanocomposites, energy storage, biosensors, and reinforcement materials in composites
Fullerenes	Spherical carbon molecules with cage-like structures	Unique molecular symmetry, high electron affinity, and potential as electron acceptors in organic photovoltaic devices	Drug delivery systems, antioxidants, lubricants, and superconductors
Carbon Nanodots (CNDs)	Small carbon nanoparticles with sizes less than 10 nm	Excellent photoluminescence, biocompatibility, low toxicity, and tunable optical properties	Bioimaging, sensing, drug delivery, optoelectronic devices, and photocatalysis
Carbon Nanofibers (CNFs)	Fibrous carbon nanostructures with diameters ranging from tens to hundreds of nanometers	High tensile strength, flexibility, and excellent electrical and thermal conductivity	Aerospace materials, reinforcement materials in composites, energy storage, electrodes in batteries and supercapacitors, and tissue engineering scaffolds
Graphitic Carbon Nitride (g-C3N4)	Layered carbon nitride materials with graphitic structure	Visible-light photocatalytic activity, chemical stability, and high surface area	Photocatalysis for water splitting, pollutant degradation, hydrogen evolution, and organic synthesis

such as Integrated Coal Gasification Combined Cycle (IGCC) and Integrated Gasification Fuel Cell Cycle (IGFC) provide opportunities for increased efficiency and virtually complete elimination of harmful emissions into the atmosphere. This is achieved through the utilization of fuel cells, gasifiers, oxygen blowing processes, and other technologies. As a result of such processes, it is possible to obtain carbon nanomaterials, which can be used for hydrogen storage. Additionally, these technologies enable the production of hydrogen in quantities up to 85% (for IGCC, IGFC technologies) (Graifer et al., 2011; Yermagambet et al., 2020). The aim of this study is to synthesize graphene-like carbon nanomaterials via arc discharge method from graphite rods and investigate their physicochemical and electrophysical properties.

MATERIALS & METHODS

In this study, graphene-like nanomaterials were synthesized using a laboratory arc discharge chamber developed by the Institute of Coal Chemistry and Technology, Astana, Kazakhstan. The arc discharge method for obtaining graphene and graphene-containing materials offers several advantages. In particular, it is characterized by low production cost, high efficiency, and the ability to synthesize without the use of a catalyst. This method is easily applicable in laboratory conditions and can be scaled up for industrial production (Yermagambet et al., 2021).

The essence of the method lies in the thermal spraying of a graphite electrode in the plasma of an arc discharge occurring in an inert gas atmosphere (Graifer et al., 2011). The synthesized graphene and graphene-containing materials are formed both on the inner surface of the reactor and on the electrode surface. The chamber, as depicted in (Fig. 1), consists of two horizontally mounted electrodes. After turning on the power supply (DC), the electrodes are brought close to each other, forming an arc, and maintained with an intermittent gap of 1-2mm for stable discharge. Graphite electrodes are placed in a chamber filled with an inert nitrogen atmosphere, and the current strength at a constant voltage of 75V ranges from 50 to 400A in increments of 50A. The arc current generates plasma with a very high temperature of about 4000-6000K, leading to carbon sublimation. Carbon vapors aggregated in the gas phase are directed towards the cathode, where they are cooled due to the temperature gradient. After arc action lasts for several minutes, the discharge is stopped, and the cathodic deposit containing graphene-like materials is collected from the chamber walls. These deposits then undergo further purification and are examined under an electron microscope to study their morphology.

The investigation of carbon modification type was carried out using the method of Raman scattering. Spectra of samples were recorded on the Integra Spectra scanning probe microscope using a laser with a wavelength of 473nm. Raman scattering enables the determination of the chemical structure and functional groups in the samples. The quality of carbon materials was assessed using the intensity ratio of I_D/I_G. Then, the intensity ratio of I_{2D}/I_G is calculated to characterize the formation of mono- and multilayer graphene or carbon nanotubes.

The study of the structure and dimensionality of carbon nanomaterials was conducted using the energy-dispersive X-ray spectroscopy method on the scanning electron microscopy (SEM) instrument (Quanta 3D 200i) with an attachment for energy-dispersive analysis from EDAX. This method allows for the analysis of the elemental composition of samples based on their X-ray spectrum. The specific surface area and specific pore volume by the method of Brunauer-Emmett-Teller (BET) were studied using the KATAKON Sorbtometer M apparatus. The BET method is used to determine the pore parameters of materials. To determine the electrophysical characteristics, such as dielectric permittivity (ε) and electrical resistance (R), the capacitance (C) of samples was measured on the LCR-800 serial instrument (measuring L, C, R) at frequencies of 1, 5 and 10kHz with a basic accuracy of 0.05-0.1%.

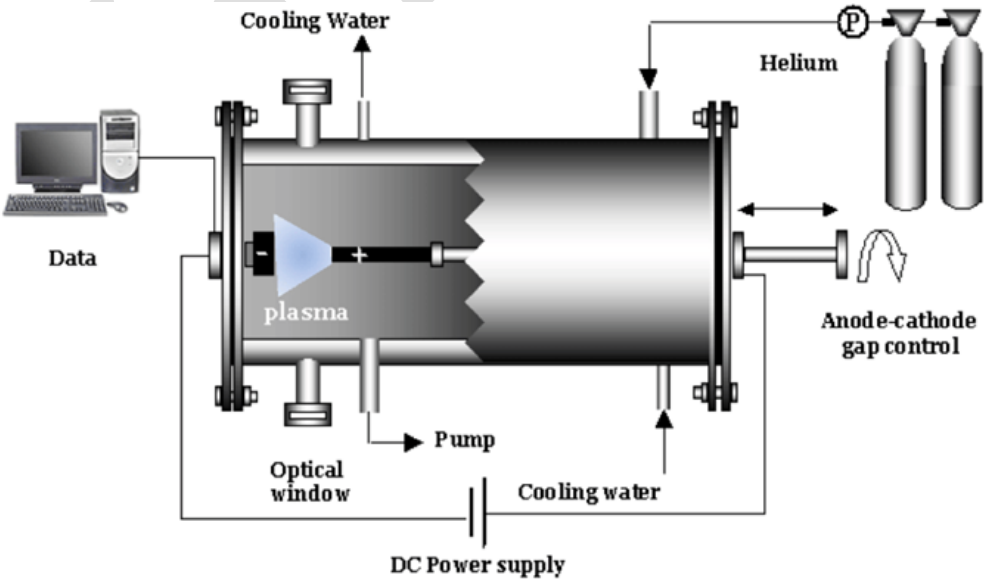

Fig. 1: Schematic representation of a arc discharge chamber used for the synthesis of graphene-like materials.

The comparative calculation method of Lotte-Karapetian was applied to assess the temperature dependence of the electrophysical properties of the investigated objects (Karapetyants, 1965). For this purpose, the electrical resistance values of barium titanate ($BaTiO_3$) and the investigated objects were used in the temperature range from 293 to 483K and at frequencies of 1, 5, and 10kHz. The main reference point was the specific resistance value of $BaTiO_3$ at room temperature, which was 1010Ohm·cm. The calculation was performed according to the corresponding methodology (Venevtsev, 1985):

$$\frac{R_{\mathrm{BaTiO_3}}}{R_{\mathrm{sp.BaTiO_3}}} = \frac{R_{\mathrm{material}}}{R_{\mathrm{sp.material}}} \quad (1)$$

Values of electrical resistance for all temperatures (Rsp.) and frequencies are likewise calculated, using a similarity coefficient of 0.0754, which considers the experimental resistance values of the material at corresponding temperatures (R). Subsequently, the specific electrical conductivity of the materials (Ohm-1·m-1) was determined from the values of specific electrical resistance of the investigated materials using Formula 2 (Kudryashov et al., 1991):

$$\chi = \frac{1}{\rho} \quad (2)$$

RESULTS & DISCUSSION

Graphene, obtained during this study, possesses the following characteristics (%): moisture content (Wr) - 0.14; absolute density (Ad) - 42.54; volatile matter content (Vdaf) - 29.38.

The Raman spectroscopy results of the carbon materials obtained during the present study are presented below (Fig. 2). They demonstrate characteristic D, G, and G' (or 2D) peaks in all samples. The D peak corresponds to disorder or defects in the graphite structure, often referred to as sp3 C–C bonds, while the G band represents in-plane stretching vibrations of sp2 carbon atoms. A broad D-band peak indicates that the sample contained a relatively large amount of disordered structure and defects. Additionally, the 2D peak in the Raman spectrum of the sample characterizes the formation of carbon nanotubes or graphene (Rotenberg, 2000).

The Raman spectroscopy spectrum of the first sample exhibits signals with characteristic D and G peaks (1362cm^{-1} and 1574cm^{-1}). The D band indicates disordered structure and defects associated with amorphous carbon, while the G band suggests stretching of sp2 C–C bonds. Additionally, the sample's Raman spectrum shows a 2D peak at 2714cm^{-1}, indicating the formation of carbon nanotubes or graphene. The degree of graphitization and peak ratios depend significantly on the spectral decomposition method – Gaussian or Lorentzian, as well as the choice of the G peak position (Fesenko, 1972). The obtained samples exhibited high degrees of orderliness and long-range structure (2D peak). These samples have spectra similar to graphite-like materials, such as carbon nanotubes or graphene. Table 2 presents the dependencies of the degree of graphitization (Gf), the intensity ratios of I(G)/I(2D) and I(G)/I(D) on the current strength during the synthesis of carbon nanomaterials.

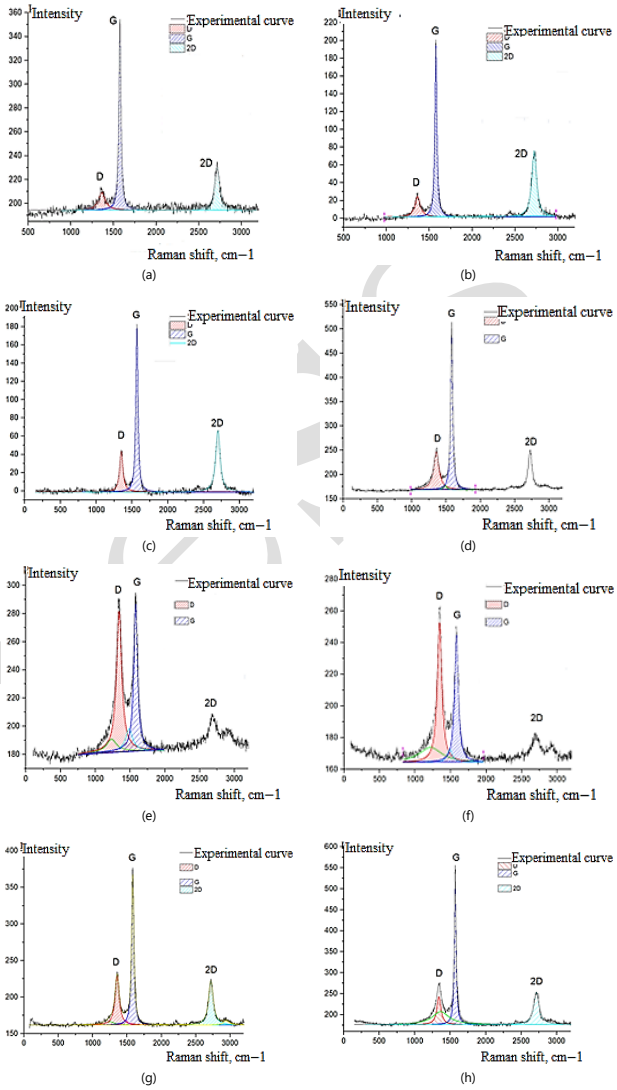

Fig. 2: The Raman spectroscopy results of the carbon materials obtained by the arc discharge method at currents equal to: (a) 50A; (b) 100A; (c) 150A; (d) 200A; (e) 250A; (f) 300A; (g) 350A; and (h) 400A.

Table 2: Raman Spectroscopy Results of Carbon Nanomaterials

Characteristics of Carbon Nanomaterials:	Current strength, A							
	50	100	150	200	250	300	350	400
Gf, %	75.54	75.14	71.63	59.9	35.3	31.7	56.83	43.87
I(G)/I(2D)	4.35	2.60	2.73	3.60	5.16	3.58	3.36	4.53
I(G)/I(D)	10.79	8.39	4.12	2.33	1.04	2.63	3.05	11.36
I(D)/I(G)	0.09	0.12	0.24	0.23	0.96	1.14	0.33	0.09
I(2D)/I(G)	0.23	0.38	0.37	0.24	0.19	0.17	0.29	0.22

In the first case, the I2D/IG intensity ratio is 0.23, indicating a multilayer structure of the material. Similarly, the IG/I2D intensity ratio of 4.35 suggests the multilayer nature of the nanomaterial. The ID/IG intensity ratio of 0.09 indicates a low level of defects in the considered material. Thus, the degree of graphitization is estimated to be 75.54%.

The Raman spectra effectively delineate the structural nuances of graphene-based materials. The position of the 2D peak in the spectrum, typically situated within the

range of ~2685-2724 cm^{-1}, allows inference regarding the presence of multilayer graphene and graphene-containing compounds. The values of the intensity ratio between the peaks I2D/IG, spanning from 0.17 to 0.38, suggest a predominant formation of three- or four-layer graphene. Analysis of the intensity ratio between peaks G and 2D also corroborates the existence of both single- and multilayer graphene. For example, IG/I2D values ranging from 2.60 to 5.16 imply the presence of two to five layers of graphene (for monolayer graphene, this ratio typically exceeds 0.6-1).

These deductions stem from variations in the position and intensity of the 2D peak in the Raman spectra, indicative of the presence of multilayer graphene structures. Monolayer graphene typically exhibits a 2D peak at approximately 2679cm-1, whereas multilayer graphene displays a shift towards higher wavenumbers along with broadening. Moreover, the intensity ratio I2D/IG varies across different graphene layers: monolayer graphene usually exceeds 1.6, bilayer graphene approximately 0.8, trilayer graphene around 0.30, and multilayer graphene (more than 4 layers) approximately 0.07.

The relative intensity ratio between the D and G bands (ID/IG) serves as a crucial metric for evaluating the quality of carbonaceous materials. The observed values within the range of 0.09 to 1.14 suggest a significant presence of defects within the material. The degree of graphitization (Gf), estimated within the range of 31.70 to 75.54%, indicates a reduction in graphitization with increasing current strength, albeit with a reversed trend at 350 and 400A. Maximum graphitization content is noted in samples synthesized at current strengths of 50, 100, 150, and 200A.

Fig. 3 presents the scanning electron microscopy (SEM) analysis results of the carbon materials. Scanning electron microscopy analysis of the carbon material formed in the reactor revealed the formation of flake-like carbon particles. These are likely carbon nanotubes or graphene-containing nanomaterials. The particle sizes ranged from 64.2 to 69.9nm.

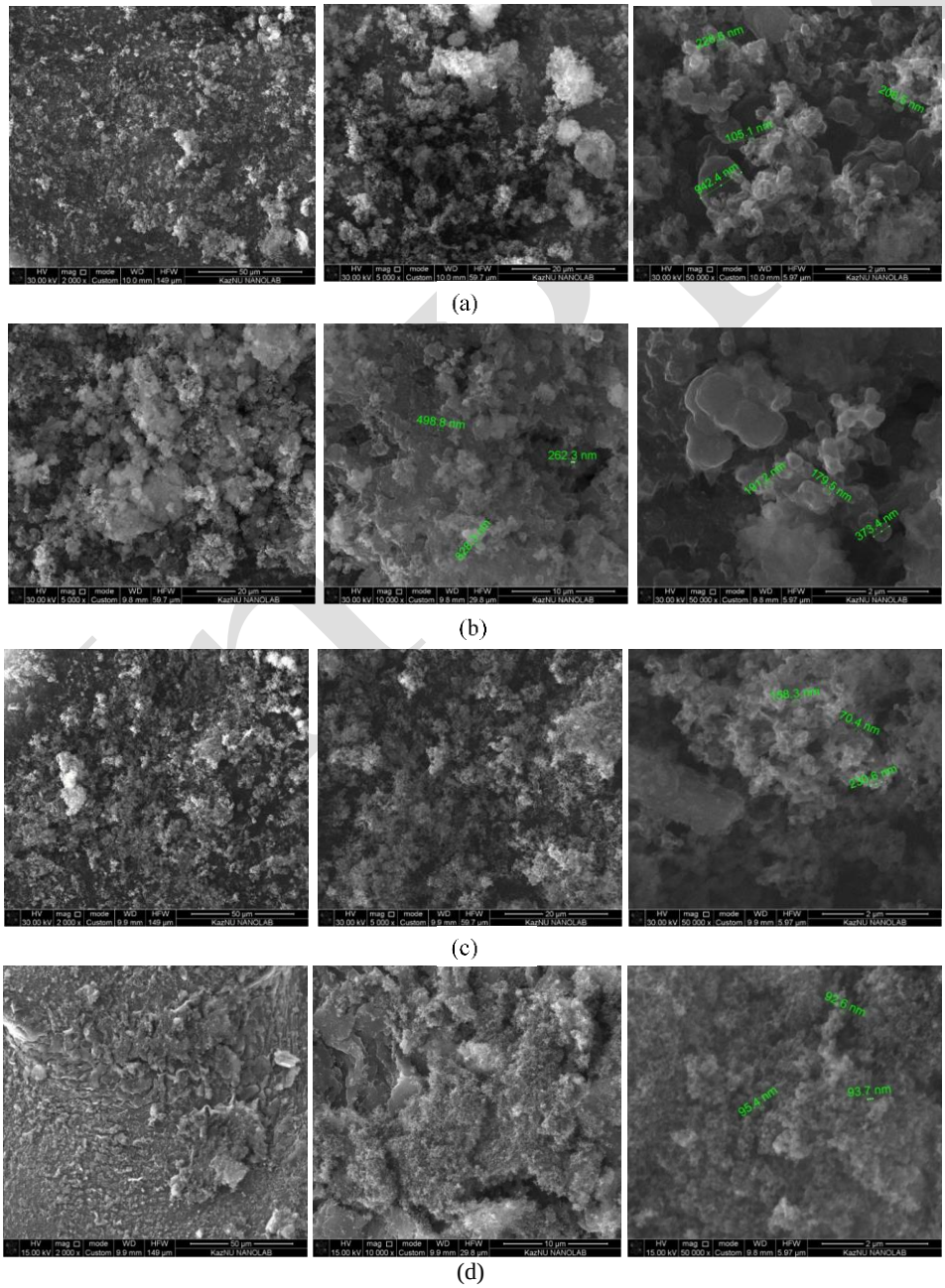

Fig. 3: Scanning electron microscopy (SEM) imaging of the carbon materials obtained by the arc discharge method at currents equal to: (a) 50A; (b) 100A; (c) 150A; (d) 200A.

Further SEM imaging revealed the presence of delicate graphene sheets. The morphology of these graphene sheets, formed under a nitrogen inert atmosphere, exhibited similarities across samples obtained at current strengths of 50, 100, 150, and 200A. The appearance resembled naturally crumpled and contoured petals, with dimensions ranging from 105 to 942nm at 50A, from 179 to 828nm at 100A, from 70 to 230nm at 150A and from 92 to 95nm at 200A. Agglomeration of these graphene petals was observed, possibly due to their diminutive size. Surface imperfections in the graphene sheets, characterized by surface folds, contributed to their varied levels of transparency. Table 3 presents the specific surface area and specific pore volume of the samples.

Table 3: Specific surface area and specific pore volume of the samples obtained at currents ranging from 50 to 200A

Current, A	Specific Surface Area, m^2/g	Specific Pore Volume, cm^3/g
50	26.580	0.011
100	56.203	0.024
150	159.737	0.068
200	140.143	0.060

The specific surface area, determined by BET model, was 26.58m^2/g for the sample synthesized via arc discharge at a current strength of 50A, approximately six times lower than that at 150A. An increase in both specific surface area and specific pore volume was observed with escalating current strength, with a marginal decline at 200A. Table 4 presents the results of measuring the electrophysical characteristics of the original graphite.

The results presented in Table 4 demonstrate that within the considered temperature range (293-483K), the graphite sample's conductivity varies significantly with frequency. For instance, at 1kHz and 293K, its value is 6.07×10^7, which increases to 7.2×10^8 at 453K and further to 483K, exceeding the measurement instrument's capabilities. With an increase in frequency to 5 and 10kHz, the values of electrical permittivity (ε) decrease but remain sufficiently high: 4.04×10^6 (293K) and 2.56×10^8 (483K) at 5kHz, as well as 1.15×10^6 (293 K) and 8.71×10^7 (483K) at 10kHz.

Investigation of the dependence of electrical resistance (R) on temperature reveals that the material exhibits semiconductor conductivity within the range of 293-483K. The width of the bandgap in this temperature range is calculated as follows (Morachevsky & Sladkov, 1985):

$$\Delta E = \frac{2 \times 0{,}000086173 \times 293 \times 483}{0{,}43(483 - 293)} lg \frac{3{,}44}{2{,}34} = 0{,}44eV \qquad (3)$$

The research findings indicate that the bandgap width of original graphite in the temperature range from 293 to 483K is 0.44eV, classifying it as a narrow-bandgap semiconductor.

The results of barium titanate (BaTiO3) measurement, needed to validate the obtained data, demonstrated that the dielectric permittivity values at 293K and frequencies of 1kHz and 5kHz complied with the recommended range of 1400±250. Despite the decreased values at 10kHz, the dielectric permittivity of BaTiO3 remained approximately constant between 313 and 483K at all three frequencies, not exceeding 2150. This suggests that changes in frequency have minimal impact on the temperature dependence of the dielectric permittivity of BaTiO3 within this range.

Table 4: Dependence of electrical resistance (R), capacitance (C), and dielectric permeability (ε) on the temperature of graphite

T, K	C, nF	R, Ohm	ε	lgε	lgR
		Measurement Frequency 1 kHz			
293	8434.9	2738	60706754	7.78	3.44
303	7649.2	2637	55051999	7.74	3.42
313	6315.2	2435	45451078	7.66	3.39
323	5606.8	2238	40352658	7.61	3.35
333	3778.3	2111	27192774	7.43	3.32
343	2547.9	1909	18337472	7.26	3.28
353	1867.4	1643	13439850	7.13	3.22
363	1896.1	1123	13646407	7.14	3.05
373	1928.5	931.4	13879593	7.14	2.97
383	2416.7	850.1	17393213	7.24	2.93
393	7702.6	889.1	55436324	7.74	2.95
403	15766	800.5	113469358	8.05	2.90
413	24890	728.6	179135629	8.25	2.86
423	40039	643.7	288164382	8.46	2.81
433	60332	570.1	434214977	8.64	2.76
443	86570	487.8	623052287	8.79	2.69
453	99999<	398.9	719702040<	8.86<	2.60
463	99999<	332.9	719702040<	8.86<	2.52
473	99999<	275.4	719702040<	8.86<	2.44
483	99999<	218.6	719702040<	8.86<	2.34
		Measurement Frequency 5 kHz			
293	562.38	2688	4047501	6.61	3.43
303	524.51	2588	3774947	6.58	3.41
313	483.22	2407	3477779	6.54	3.38
323	420.05	2185	3023139	6.48	3.34
333	309.83	2052	2229875	6.35	3.31
343	271.41	1804	1953363	6.29	3.26
353	251.6	1503	1810788	6.26	3.18
363	311.14	1002	2239303	6.35	3.00
373	370.08	827.3	2663500	6.43	2.92
383	447.7	792.6	3222138	6.51	2.90
393	892.94	864.4	6426572	6.81	2.94
403	1584	777	11400194	7.06	2.89
413	2372.8	709.6	17077261	7.23	2.85
423	3566.5	636.7	25668430	7.41	2.80
433	5104.3	558.2	36736119	7.57	2.75
443	7413.6	478.9	53356364	7.73	2.68
453	11166	392.4	80362733	7.91	2.59
463	16061	325.9	115592501	8.06	2.51
473	23184	270.7	166857390	8.22	2.43
483	35604	216.3	256245277	8.41	2.34
		Measurement Frequency 10 kHz			
293	160.43	2666	1154630	6.06	3.43
303	155.09	2537	1116197	6.05	3.40
313	143.43	2376	1032279	6.01	3.38
323	142.58	2107	1026161	6.01	3.32
333	108.95	1963	784123	5.89	3.29
343	107.61	1709	774479	5.89	3.23
353	127.77	1125	919572	5.96	3.05
363	147.83	936.4	1063946	6.03	2.97
373	185.3	782.9	1333621	6.13	2.89
383	208.1	774.7	1497715	6.18	2.89
393	344.83	849.9	2481773	6.39	2.93
403	570.19	765.8	4103710	6.61	2.88
413	836.86	695.8	6022959	6.78	2.84
423	1187.3	621.1	8545108	6.93	2.79
433	1683.1	550.5	12113426	7.08	2.74
443	2391.8	473	17214006	7.24	2.67
453	3613.1	384.9	26003814	7.42	2.59
463	5231.6	320	37652308	7.58	2.51
473	7640.6	267	54990104	7.74	2.43
483	12099	213.4	87077621	7.94	2.33

Furthermore, investigations on the electrophysical properties of carbon materials synthesized via the arc discharge method at currents ranging from 50 to 200A, characterized by a high degree of graphitization, showed results presented in Table 5.

Table 5: Dependency of electrical resistance (R), capacitance (C), and dielectric permittivity (ε) on the temperature of the obtained materials

Material Name	Dielectric Permittivity (ε)					
	at 1kHz		at 5kHz		at 10kHz	
	293K	483K	293K	483K	293K	483K
BaTiO3	1296	2159	1220	2102	561	2100
50A	25998	215910612<	4735	83739609	2209	27038756
100A	525877	287880816<	51819	37393213	24336	11181691
150A	894332	199207600	66385	12113354	22917	3674188
200A	691022	143940408<	56025	16403613	20552	4982115
	Electrical Resistances (lgR)					
BaTiO3	4.13	3.67	4.47	3.58	5.18	3.37
50A	4.68	2.13	4.58	2.13	4.53	2.12
100A	3.98	2.35	3.92	2.35	3.85	2.34
150A	3.80	2.38	3.76	2.37	3.73	2.36
200A	4.01	2.57	3.98	2.58	3.96	2.58

The research of the temperature dependence of the dielectric permittivity (ε) of the graphite nanomaterial, obtained at a current of 50A and voltage of 75V, demonstrates that with increasing temperature, the values of dielectric permittivity increase, while they decrease with increasing frequency. The maximum values of ε at 1kHz are achieved at 453K (2.16×10^8), at 5kHz at 483K (8.37×10^7), and at 10kHz also at 483K (2.70×10^7). These values exceed the ε of the standard BaTiO3 by 114,178 times at 453K (at 1kHz), by 39,838 times at 483K (at 5kHz), and by 12,876 times at 483K (at 10kHz). The study of the temperature dependence of the electrical resistance (R) of this material shows that in the range of 293-373K it exhibits semiconductor conductivity, metallic conductivity at 373-403K, and again semiconductor conductivity at 403-483K (at 10kHz). This material is of interest as a semiconductor and as a material for microcapacitors at a temperature of 363K and in the range of 423- 483 K.

The results of the study of the temperature dependence of the dielectric permittivity (ε) of the nanomaterial obtained at a current of 100A and a voltage of 75V show that at all frequencies and in the range of 293-483K it has high values of ε. For example, at 293K, the ε values of this material exceed those of the standard BaTiO3 by 406 times at 1 kHz, by 42 times at 5 kHz and by 43 times at 10 kHz. This also proves this material's potential in microcapacitor technology application (Erin, 2009). The temperature dependence of the electrical resistance (R) of this material shows that in the range of 293-363K, it exhibits semiconductor conductivity, metallic conductivity at 363-393K, and again semiconductor conductivity at 393-483K (at 10kHz). The band gap width of this material in the range of 293-363K is 0.72eV, and at 493-483K, it is 1.2eV, classifying it as narrow-bandgap semiconductor.

The results of the analysis of the temperature dependence of the dielectric permittivity indicate high values of ε for the graphene-like nanomaterial obtained at 150A and 75V. At 293K and 483K, the ε values exceed those of the standard BaTiO3 by several orders of magnitude. An increase in ε is observed with increasing temperature, reaching values from 8.94×10^5 to 1.99×10^8 at 1kHz in the range from 293K to 483K. The study of the temperature dependence indicates that the material exhibits semiconductor conductivity in the range from 293 to 403K, metallic conductivity at 403-423K and again semiconductor conductivity at 423-483K.

For the material obtained at 200A and 75V, the ε values also significantly exceed those of the standard BaTiO3 at all tested frequencies and temperatures. A decrease in ε is observed with increasing frequency and an increase with increasing temperature. The maximum values of ε are achieved at 1kHz, being 6.91×10^5 at 293K and 1.44×108 at 483K. The study of the electrical resistance dependence shows that the material exhibits semiconductor conductivity throughout the investigated temperature range. The band gap width varies from 0.47 to 0.58eV depending on the temperature and frequency. The conclusions indicate the potential use of the obtained carbon materials in various technological applications requiring high values of dielectric permittivity and semiconductor conductivity. The comparative analysis of experimental data on electrical resistance and conductivity over a wide range of temperatures and frequencies enabled the calculation of specific electrical resistances and conductivities of carbonaceous materials. Table 6 presents the results of these calculations.

The obtained results confirm the semiconductor nature of the examined samples, rendering them attractive for semiconductor technology in novel multifunctional materials.

Of particular interest are the obtained fundamental constants, namely the specific electrical resistances and conductivities of the investigated materials. These values allow for a comparison of the effectiveness of carbonaceous materials with similar compounds, such as the new La15/8Sr1/8NiO4, which exhibits high dielectric constants in the range of 10^5-10^6.

Experimental data confirm that the arc discharge method is an effective means of producing graphene-containing materials from graphite. It ensures high purity of the product with minimal defects. The optimal synthesis parameters are 150A and 75V, providing a material with high specific surface area, dielectric permittivity, and low specific electrical resistance.

As highlighted in the reviews compiled by (Lines & Glass, 2001), graphene materials hold promise for applications in energy storage devices. For instance, supercapacitors require electrodes with high conductivity and large surface areas, making graphene suitable for this application. It is considered to be an alternative to transparent electrodes made of indium tin oxide (ITO). Graphene can also be utilized in transparent heating elements and thermoacoustic transducers. In the context of hydrogen storage, graphene offers several advantages: it is environmentally friendly (Narozhnykh et al., 2024), lightweight, thermally and chemically stable, possesses high mechanical strength, and is suitable for long-distance transportation. Furthermore, graphene is a flexible material, making it fit for various devices. Graphene synthesis is feasible in large quantities through various methods, and its production becomes increasingly accessible with each passing year.

Raman spectroscopy confirmed the formation of multilayer graphene structures with prominent D (~1362cm^{-1}), G (~1574cm^{-1}) and 2D (~2714cm^{-1}) peaks. The D-band reflects structural imperfections or sp^3 hybridized carbon, while the G-band signifies sp^2 carbon

Table 6: Specific electrical resistance (R) and specific electrical conductivity (σ) of carbon materials

T, K	R, Ohm·cm				χ, Ohm-1·m-1			
	50A	100A	150A	200A	50A	100A	150A	200A
	Measurement Frequency 1kHz							
293	3577.7	714.0	763.0	473.6	0.0280	0.1401	0.1311	0.2111
303	474.5	667.0	745.4	419.8	0.2107	0.1499	0.1342	0.2382
313	2582.5	605.3	680.7	398.7	0.0387	0.1652	0.1469	0.2508
323	947.8	510.8	634.6	369.8	0.1055	0.1958	0.1576	0.2704
333	502.7	413.3	574.3	330.3	0.1989	0.2420	0.1741	0.3028
343	286.9	307.5	511.7	264.3	0.0349	0.3271	0.1954	0.3784
353	123.9	235.9	464.5	208.9	0.0807	0.4239	0.2153	0.4787
363	61.6	177.3	342.9	162.4	1.6234	0.5640	0.2916	0.6158
373	39.7	169.0	197.8	122.4	2.5189	0.5917	0.5056	0.8170
383	53.2	189.3	152.6	119.7	1.8797	0.5283	0.6553	0.8354
393	66.0	188.4	87.5	116.6	1.5152	0.5308	1.1429	0.8576
403	63.6	173.9	78.5	92.4	1.5723	0.5750	1.2739	1.0823
413	54.0	138.6	93.2	79.1	1.8519	0.7215	1.0730	1.2642
423	42.6	114.2	92.3	65.1	2.3474	0.8757	1.0834	1.5361
433	36.0	78.3	82.0	53.4	2.7778	1.2771	1.2195	1.8727
443	27.4	58.0	67.1	43.2	3.6496	1.7241	1.4903	2.3148
453	22.3	47.5	54.6	33.8	4.4843	2.1053	1.8315	2.9585
463	17.8	33.4	43.1	26.2	5.6180	2.9940	2.3202	3.8168
473	13.5	23.5	34.0	21.3	7.4074	4.2553	2.9412	4.6948
483	10.2	17.0	28.2	17.8	9.039	5.8824	3.5461	5.6180
	Measurement Frequency 5kHz							
293	2897.6	623.9	724.0	438.5	0.0345	0.1603	0.1381	0.2281
303	3302.5	588.7	691.8	419.8	0.0302	0.1699	0.1446	0.2382
313	1736.5	513.4	628.8	398.7	0.0576	0.1948	0.1590	0.2508
323	675.1	420.1	580.4	369.8	0.1481	0.2380	0.1723	0.2704
333	368.3	341.4	520.3	330.3	0.2715	0.2929	0.1922	0.3028
343	220.6	253.2	457.6	264.3	0.4533	0.3949	0.2185	0.3784
353	114.1	195.1	402.3	208.9	0.8764	0.5126	0.2486	0.4787
363	53.2	147.3	278.2	162.4	1.8797	0.6789	0.3595	0.6158
373	37.4	146.0	164.4	122.4	2.6738	0.6849	0.6083	0.8170
383	48.1	164.8	129.1	119.7	2.0790	0.6068	0.7746	0.8354
393	60.7	171.7	75.0	116.6	1.6774	0.5824	1.3333	0.8576
403	60.6	159.4	69.4	92.4	1.6502	0.6274	1.4409	1.0823
413	52.3	128.6	86.6	79.1	1.9120	0.7776	1.1547	1.2642
423	41.9	94.1	87.5	65.1	2.3866	1.0627	1.1429	1.5361
433	35.2	75.4	78.6	53.4	2.8409	1.3263	1.2723	1.8727
443	26.9	55.9	64.3	43.2	3.7175	1.7889	1.5552	2.3148
453	21.7	45.9	53.0	33.8	4.6083	2.1786	1.8868	2.9586
463	17.3	32.4	41.9	26.2	5.7803	3.0864	2.3866	3.8168
473	13.4	22.5	33.3	21.3	7.4669	4.4444	3.0030	4.6948
483	10.1	16.7	28.9	17.8	9.9010	5.9880	3.4602	5.6180
	Measurement Frequency 10kHz							
293	2567.4	533.8	683.3	405.9	0.0389	0.1873	0.1463	0.2464
303	2656.3	511.9	652.5	388.7	0.0376	0.1954	0.1533	0.2573
313	1255.4	448.1	595.3	364.6	0.0797	0.2232	0.1680	0.2743
323	557.6	368.3	538.3	336.5	0.1793	0.2715	0.1858	0.2972
333	310.2	295.6	481.4	294.7	0.3224	0.3383	0.2077	0.3393
343	195.0	224.1	426.7	233.7	0.5128	0.4462	0.2344	0.4279
353	112.1	174.2	364.1	182.3	0.8921	0.5740	0.2747	0.5485
363	44.1	132.5	243.6	142.1	2.2676	0.7547	0.4105	0.7037
373	37.5	135.3	147.6	109.0	2.6667	0.7391	0.6775	0.9174
383	46.5	150.6	93.5	110.6	2.1505	0.6640	1.0695	0.9042
393	58.2	160.7	69.9	108.1	1.7182	0.6222	1.4306	0.9251
403	58.2	148.8	65.3	88.4	1.7182	0.6720	1.5314	1.1312
413	50.7	121.1	82,9	76.2	1.9724	0.8258	1.2063	1.3123
423	40.78	90.6	83.9	63.3	2.4522	1.1038	1.1919	1.5798
433	34.3	72.2	75.9	52.0	2.9155	1.3850	1.3575	1.9231
443	26.5	57.8	62.1	42.2	3.7736	1.8248	1.6103	2.3697
453	21.2	44.5	51.5	33.0	4.7170	2.2472	1.9417	3.0303
463	17.2	31.7	40.9	28.8	5.8140	3.1546	2.4450	3.8760
473	13.1	21.9	32.7	20.8	7.6336	4.5662	3.0581	4.8077
483	9.9	16.5	28.7	17.5	10.1010	6.0606	3.4843	5.7143

lattice vibrations, characteristic of high-quality graphene derivatives (Ferrari & Basko, 2013; Su & Hu, 2020). The 2D peak's position and intensity (I_2D/I_G ratio ~0.23) indicate the predominance of multilayer graphene, aligning with prior studies that report similar spectral features for arc-synthesized graphene (Su & Zhang, 2014; Schuepfer et al., 2020). The low I_D/I_G ratio (~0.09) confirms minimal defects, demonstrating a high degree of graphitization (~75%), essential for electrical performance and material reliability (Wang et al., 2022).

SEM analyses revealed characteristic petal-like graphene morphologies with flake sizes between ~70–942nm. Such nanoscale morphology, featuring wrinkled and folded sheets, increases the active surface area—a key parameter for soil moisture sensing applications where material-soil interaction is critical (Su et al., 2021). BET results showed a specific surface area peaking at ~159.7m^2/g, corroborating earlier reports of arc-discharge-derived graphene-like materials. The electrical resistance (R) and conductivity profiles revealed that the materials exhibit semiconductor behavior across 293–483K, with a transition to metallic conductivity at mid-temperature ranges (373–423K). Narrow bandgaps (0.44–1.2eV) were calculated, consistent with graphene's reported semiconducting characteristics when synthesized with controlled defect densities (Xu et al., 2020). This tunable conductivity is crucial for resistive soil sensors, offering high sensitivity to environmental changes (Ghaffarkhah et al., 2021). The integration of graphene-like nanomaterials with high dielectric permittivity and tunable conductivity can markedly enhance soil moisture sensors' sensitivity and accuracy. Traditional soil sensors based on ceramic or polymer materials often face limitations in sensitivity under varying environmental conditions (Santhosh & Park, 2023). In contrast, the graphene-like materials synthesized in this study not only demonstrate superior dielectric behavior but also sustain electrical stability over a wide temperature range, making them robust candidates for field-deployable agricultural sensors (Wang et al., 2022).

Additionally, the unique nanostructures observed-comprising crumpled and wrinkled graphene sheets—provide enhanced soil contact area, improving signal transduction efficiency in capacitive sensing (Shoukat et al., 2024). The arc discharge method proved highly effective for producing graphene-like materials with low defect densities and high crystallinity. This method is advantageous compared to chemical vapor deposition (CVD) and chemical exfoliation techniques due to its simplicity, high yield, and cost-effectiveness (Wei et al., 2019). Recent studies have also emphasized arc discharge's eco-friendliness and scalability, crucial for real-world sensor development (Shoukat et al., 2024).

Conclusion

The study aimed to analyze the structural and electrophysical characteristics of carbon nanomaterials synthesized using the arc discharge method at various current values. Spectroscopic analysis using Raman spectroscopy confirmed the formation of multilayer graphene. Evaluation of graphitization degree indicated a decrease in graphitization with increasing current, except for cases of 350 and 400A currents. Morphological analysis of graphene sheets using scanning electron microscopy revealed the presence of lightweight graphene sheets with surface wrinkles. Although further investigation employing techniques such as transmission electron microscopy

(TEM), atomic force microscopy (AFM), and scanning tunneling microscopy (STM) is required to ascertain the number of layers in the planar graphene sheets. Specific surface area and pore volume increased with increasing current, except for a slight decrease at 200A. The obtained results provide deeper insights into the formation processes and properties of carbon nanomaterials.

Semiconductor Nature of Carbon Materials: The results of the investigations into the temperature dependence of electrical resistance and dielectric permeability confirm that the examined samples possess semiconductor properties. This renders them attractive for application in semiconductor technology for the development of new multifunctional materials.

High Dielectric Permittivity Values: The studies have shown that carbon materials exhibit high values of dielectric permeability at various frequencies and temperatures. This indicates their potential for application in various electronic and electrical devices where high dielectric permeability is required.

Efficiency of the Arc Discharge Method: Experimental data confirm that the arc discharge method is an efficient means of obtaining graphene-containing materials from graphite. It ensures high purity of the produced material with minimal defects, making it attractive for a wide range of industrial and scientific applications.

Application Perspectives: Research indicates the potential of carbon materials in various technological fields such as energy storage, supercapacitor development, transparent heating elements, and thermoacoustic converters. These materials may also find application in hydrogen storage and other promising technologies.

Further Research: Further investigations are necessary for a deeper understanding of the properties of carbon materials and to fully exploit their potential for specific applications. This includes studying the structure, morphology, and electronic properties of the materials, as well as developing new synthesis methods and improving existing technologies.

DECLARATIONS

Funding: This research has been funded by the Science Committee of the Ministry of Science and Higher Education of the Republic of Kazakhstan (Grant No. AP19577512 "Development of scientific and technical bases for obtaining microporous carbon nanomaterials for hydrogen separation and storage").

Acknowledgement: The authors would like to express their sincere gratitude to the editor of the journal and the anonymous reviewers for their valuable comments and constructive suggestions, which have significantly contributed to the improvement of this article

Conflicts of Interest: Authors declare no conflict of interest.

Data Availability: The data is available upon request from the corresponding author.

Ethics Statement: This research did not involve human participants or animals and thus did not require formal ethical approval. All experimental procedures were conducted in accordance with institutional and national guidelines for scientific research.

Author's Contributions: M.K. Kazankapova: Conceptualization, methodology development, supervision, and writing – original draft preparation; B.T. Yermagambet: Experimental design, data analysis, and interpretation; B.K. Kasenov: Electrophysical testing, dielectric property evaluation; A.B. Malgazhdarova: BET surface area and pore volume analysis, visualization; Zh.T. Dauletzhanova: Raman spectroscopy, spectral data interpretation; Zh.M. Kasenova: Arc discharge synthesis, materials characterization, Electrophysical testing, dielectric property evaluation; G.K. Mendaliyev: SEM imaging and morphological analysis; A.S. Akshekina: Literature review, reference management, and manuscript editing.

Generative AI Statement: The authors declare that no Gen AI/DeepSeek was used in the writing/creation of this manuscript.

Publisher's Note: All claims stated in this article are exclusively those of the authors and do not necessarily represent those of their affiliated organizations or those of the publisher, the editors, and the reviewers. Any product that may be evaluated/assessed in this article or claimed by its manufacturer is not guaranteed or endorsed by the publisher/editors.

REFERENCES

Abdullayev, I., Kukhar, V., Akhmetshin, E., Bekjanov, D., & Carballo-Penela, A. (2023). Preface. *E3S Web of Conferences, 449*, Article 00001. https://doi.org/10.1051/e3sconf/202344900001

Allen, M.J., Tung, V.C., & Kaner, R.B. (2010). Honeycomb carbon: A review of graphene. *Chemical Reviews, 110*(1), 132-145. https://doi.org/10.1021/cr900070d

Baibussenov, K.S. (2023). Environmental factors' influence on the diamondback moth (*Plutella xylostella* l.) population dynamics on cruciferous crops. *SABRAO Journal of Breeding and Genetics*, *55*(6), 2077–2091. https://doi.org/10.54910/sabrao2023.55.6.20

Balandin, A.A., Ghosh, S., Bao, W., Calizo, I., Teweldebrhan, D., Miao, F., & Lau, C.N. (2008). Superior thermal conductivity of single-layer graphene. *Nano Letters, 8*(3), 902-907. https://doi.org/10.1021/nl0731872

Benayad, A., Shin, H.J., Park, H.K., Yoon, S.M., Kim, K.K., Jin, M.H., Jeong, H.K., Lee, J.C., Choi, J.Y., & Lee, Y.H. (2009). Controlling work function of reduced graphite oxide with Au-ion concentration. *Chemical Physics Letters, 475*(1-3), 91-95. https://doi.org/10.1016/j.cplett.2009.05.023

Bugubaeva, A., Kuprijanov, A., Chashkov, V., Kuanyshbaev, S., Valiev, K., Mamikhina, S., Shcheglov, A., Nugmanov, A., Bulaev, A., Sultangazina, G., Kunanbayev, K., Chernyavskaya, O., Baubekova, G., Ruchkina, G., Safronova, O., Uxikbayeva, M., & Sokharev, Y. (2023). Productivity assessment of various plant communities at uranium mine sites in Central Kazakhstan. *SABRAO Journal of Breeding and Genetics, 55*(3), 864-876. http://doi.org/10.54910/sabrao2023.55.3.21

Dreyer, D.R., Park, S., Bielawski, C.W., & Ruoff, R.S. (2010). The chemistry of graphene oxide. *Chemical Society Reviews, 39*, 228-240.

Du, X., Skachko, I., Barker, A., & Andrei, E.Y. (2008). Approaching ballistic transport in suspended graphene. *Nature Nanotechnology, 3*(8), 491-495. https://doi.org/10.1038/nnano.2008.199

Eda, G., Fanchini, G., & Chhowalla, M. (2008). Large-area ultrathin films of reduced graphene oxide as a transparent and flexible electronic material. *Nature Nanotechnology, 3*(5), 270-274. https://doi.org/10.1038/nnano.2008.83

Erin, Y. (2009). A substance with a gigantic value of dielectric constant was

found. *Chemistry and Chemists, 1*, 16.

Ferrari, A.C., & Basko, D.M. (2013). Raman spectroscopy as a versatile tool for studying the properties of graphene. *Nature Nanotechnology*, *8*(4), 235–246. https://doi.org/10.1038/nnano.2013.46

Fesenko, E.G. (1972). *The perovskite family and ferroelectricity*. Moscow: Atomizdat.

Georgakilas, V., Tiwari, J.N., Kemp, K.C., Perman, J.A., Bourlinos, A.B., Kim, K.S., & Zboril, R. (2016). Noncovalent functionalization of graphene and graphene oxide for energy materials, biosensing, catalytic, and biomedical applications. *Chemical Reviews, 116*(9), 5464-5519. https://doi.org/10.1021/acs.chemrev.5b00620

Ghaffarkhah, A., Hosseini, E., Kamkar, M., Sehat, A.A., Dordanihaghighi, S., Allahbakhsh, A., Kuur, C.V.D., & Arjmand, M. (2021). Synthesis, Applications, and Prospects of Graphene Quantum Dots: A Comprehensive Review. *Small, 18*(2). https://doi.org/10.1002/smll.202102683

Graifer, E.D., Makotchenko, V.G., Nazarov, A.S., Kim, S.D., & Fedorov, V.E. (2011). Graphene: Chemical approaches to synthesis and modification. *Uspekhi Khimii, 80*(8), 784-804.

Gupta, P., Kumar, D., Quraishi, M.A., & Parkash, O. (2016). Metal matrix nanocomposites and their application in corrosion control. In Husain M., & Khan Z. (Eds.), *Advances in Nanomaterials* (Vol. 79). Springer, New Delhi. https://doi.org/10.1007/978-81-322-2668-0_6

Hersam, M. (2008). Progress towards monodisperse single-walled carbon nanotubes. *Nature Nanotechnology, 3*, 387-394. https://doi.org/10.1038/nnano.2008.135

Jariwala, D., Srivastava, A., & Ajayan, P.M. (2011). Graphene synthesis and band gap opening. *Journal of Nanoscience and Nanotechnology, 11*, 6621-6641.

Karapetyants, M.K. (1965). *Methods for comparative calculation of physical and chemical properties*. Moscow: *Khimiya*.

Kazankapova, M.K., Yermagambet, B.T., Kassenova, Z.M., & Nauryzbayeva, A.T. (2020). Electrophysical properties of carbon material based on coal of "Saryadyr" deposit. *News of the National Academy of Sciences of the Republic of Kazakhstan, Series of Geology and Technical Sciences, 3*(441), 117-125. https://doi.org/10.32014/2020.2518-170X.62

King, J.A., Klimek, D.R., Miskioglu, I., & Odegard, G.M. (2013). Mechanical properties of graphene nanoplatelet epoxy composites. *Journal of Applied Polymer Science, 128*, 4217-4223. https://doi.org/10.1002/app.38645

Kong, B., Geng, J., & Jung, H. (2009). Layer-by-layer assembly of graphene and gold nanoparticles by vacuum filtration and spontaneous reduction of gold ions. *Chemical Communications*, 2174-2176. https://doi.org/10.1039/B821920F

Kratschmer, W., Lamb, L.D., & Fostiropoulos, K. (1990). Solid C60: A new form of carbon. *Nature, 347*, 354-358.

Kudryashov, I.V., & Karetnikov, G.S. (1991). *Collection of examples and problems in physical chemistry*. Moscow: Higher School.

Lines, M. E., & Glass, A. M. (2001). *Principles and applications of ferroelectrics and related materials*. OUP Oxford.

Mazina, A., Syzdykova, D., Myrzhykbayeva, A., Raikhanova, G., & Nurgaliyeva, A. (2022). Impact of green fiscal policy on investment efficiency of renewable energy enterprises in Kazakhstan. *International Journal of Energy Economics and Policy, 12*(5), 491-497.

Markhayeva, B.A., Ibrayev, A.S., Beisenova, M., Serikbayeva, G., & Arrieta-López, M. (2023). Green Banking Tools for the Implementation of a State's Environmental Policy: Comparative StudyThe active implementation of climate change projects, the latest resource- and nature-saving technologies, and environmental measures for the green growth of na. *Journal of Environmental Management and Tourism*, *14*(1), 160-167. https://doi.org/10.14505/jemt.14.1(65).15

Morachevsky, A.S., & Sladkov, I.B. (1985). *Thermodynamic calculations in metallurgy*. Moscow: Metallurgy.

Naik, B., Hazra, S., Prasad, V.S., & Ghosh, N.N. (2011). Synthesis of Ag nanoparticles within the pores of SBA-15: An efficient catalyst for reduction of 4-nitrophenol. *Catalysis Communications, 12*, 1104-1108.

Narozhnykh, K.N., Petukhov, V.L., Syso, A.I., Konovalova, T.V., Korotkevich, O.S., & Sebezhko, O.I. (2024). Specific of accumulation of manganese in organs and tissues of Hereford cattle. *Brazilian Journal of Biology, 84*, e282174. https://doi.org/10.1590/1519-6984.282174

Nie, X., Jiang, J.C., Meletis, E.I., Tung, L.D., & Spinu, L. (2003). Synthesis, structure, and magnetic properties of ε-Co nanocrystalline thin films and annealing effects. *Journal of Applied Physics, 93*, 4750-4755. https://doi.org/10.1063/1.1561590

Nosova, S.S., Meshkov, S.A., Stroev, P.V., Meshkova, G.V., & Boyar-Sozonovitch, A.S. (2018). Digital technologies as a new vector in the growth of innovativeness and competitiveness of industrial enterprises. *International Journal of Civil Engineering and Technology, 9*(6), 1411-1422.

Palmero, P., Kern, F., Sommer, F., Lombardi, M., Gadow, R., & Montanaro, L. (2014). Issues in nanocomposite ceramic engineering: Focus on processing and properties of alumina-based composites. *Journal of Applied Biomaterials and Functional Materials, 12*(3), 113.

Raccichini, R., Varzi, A., Passerini, S., & Scrosati, B. (2014). The role of graphene for electrochemical energy storage. *Nature Materials, 14*(3), 271-279. https://doi.org/10.1038/nmat4170

Rao, C.N., Sood, A.K., Subrahmanyam, K.S., & Govindaraj, A. (2009). Graphene: The new two-dimensional nanomaterial. *Angewandte Chemie (International Edition), 48*(42), 7752-7777. https://doi.org/10.1002/anie.200901678

Richter, H., Labrocco, Grieco, W.J. (1997). Generation of higher fullerenes in flames. *The Journal of Physical Chemistry B, 101*(9), 1556-1560.

Rotenberg, B.A. (2000). *Ceramic capacitor dielectrics*. St. Petersburg: Printing House of JSC Research Institute "Girikond".

Santhosh, M., & Park, T. (2023). μPED based electrode modified with nanocomposite for the detection of proline: An abiotic stress biomarker in plant. *Precision Agriculture Science and Technology*, *5*(3), 153–161. https://doi.org/10.12972/pastj.20230012

Schuepfer, D.B., Badaczewski, F., Guerra, J.M., Hofmann, D.M., Heiliger, C., Smarsly, B., & Klar, P.J. (2020). Assessing the structural properties of graphitic and non-graphitic carbons by Raman spectroscopy. *Carbon*, *161*, 359–372. https://doi.org/10.1016/j.carbon.2019.12.094

Shavelkina, M.B., Amirov, R.K., Kavyrshin, D.I., & Yusupov, D.I. (2019). Plasma-chemical synthesis of graphene/copper nanocomposite. *Uspekhi Prikladnoi Fiziki, 7*(2), 97.

Shoukat, A., Pitann, B., Zafar, M.M., Farooq, M.A., Haroon, M., Nawaz, A., Wahab, S.W., & Saqib, Z.A. (2024). Nanotechnology for climate change mitigation: Enhancing plant resilience under stress environments. *Journal of Plant Nutrition and Soil Science*, *187*(5), 604–620. https://doi.org/10.1002/jpln.202300295

Su, H., & Hu, Y.H. (2020). Recent advances in graphene-based materials for fuel cell applications. *Energy Science & Engineering*, *9*(7), 958–983. https://doi.org/10.1002/ese3.833

Su, Y., & Zhang, Y. (2014). Carbon nanomaterials synthesized by arc discharge hot plasma. *Carbon*, *83*, 90–99. https://doi.org/10.1016/j.carbon.2014.11.023

Su, Y., Zheng, L., Yao, D., Zhang, X., Chen, H., & Xu, H. (2021). Robust physiological signal monitoring by a flexible piezoresistive sensor microstructured with filamentating laser pulses. *Sensors and Actuators A Physical*, *331*, 112907. https://doi.org/10.1016/j.sna.2021.112907

Tulepova, G., Makhashov, E., Loukia, L., Nurkhojayev, N., & Sadiev, S. (2024). Developing a nano platform for bovine brucellosis diagnostic product. *Advanced Life Sciences, 11*(2), 533-538.

Ugarte, D. (1992). Curling and closure of graphitic networks under electron-beam irradiation. *Nature, 359*, 707-709.

Venevtsev, Y.N., Politova, E.D., & Ivanov, S.A. (1985). *Ferro- and antiferroelectrics of the barium titanate family*. Moscow: Chemistry.

Wang, Y., Zhao, Y., Li, X., Jiang, L., & Qu, L. (2022). Laser-Based Growth and Treatment of Graphene for Advanced Photo- and Electro-Related Device Applications. *Advanced Functional Materials*, *32*(42). https://doi.org/10.1002/adfm.202203164

Wei, N., Yu, L., Sun, Z., Song, Y., Wang, M., Tian, Z., Xia, Y., Cai, Q., Li, Y., Zhao, L., Sun, J., & Liu, Z. (2019). Scalable Salt-Templated Synthesis of Nitrogen-Doped Graphene Nanosheets toward Printable Energy Storage. *ACS Nano*, *13*(7), 7517–7526. https://doi.org/10.1021/acsnano.9b03157

Xu, W., Lan, P., Jiang, Y., Lei, D., & Yang, H. (2020). Insights into excluded volume and percolation of soft interphase and conductivity of carbon fibrous composites with core-shell networks. *Carbon*, *161*, 392–402. https://doi.org/10.1016/j.carbon.2020.01.083

Yermagambet, B.T., Kazankapova, M.K., Kasenov, B.K., Aitmagambetova, A.Z., & Kuanyshbekov, E.E. (2021). *Solid Fuel Chemistry, 55*(6), 380-390. https://doi.org/10.3103/S0361521921060057

Yermagambet, B.T., Kazankapova, M.K., Kassenova, Z.M., & Nauryzbayeva, A.T. (2020). Synthesis of carbon nanotubes by the electric arc-discharge method. *News of the National Academy of Sciences of the Republic of Kazakhstan, Series Chemistry and Technology, 5*(443), 126-133. https://doi.org/10.32014/2020.2518-1491.89

Yudasaka, M., Iijima, S., & Crespi, V.H. (2008). Single-wall carbon nanohorns and nanocones. In *Carbon Nanotubes: Synthesis, Structure, Properties and Applications* (Vol. 111, pp. 605-629). Top. Appl. Phys.

Zhang, X.X., Li, Z.Q., & Wen, G.H. (2001). Microstructure and growth of bamboo-shaped carbon nanotubes. *Chemical Physics Letters, 333*, 509-514.